Typeset using LaTeX default style in AASTeX62

Draft version May 27, 2020

Wave Polarization Analysis of the Alfvénic Slow Solar Wind at Kinetic Scales

Daniele Telloni,[1] Roberto Bruno,[2] Raffaella D'Amicis,[2] Francesco Carbone,[3] Rossana De Marco,[2] and Denise Perrone[4]

[1] *National Institute for Astrophysics - Astrophysical Observatory of Torino*
Via Osservatorio 20, 10025 Pino Torinese, Italy
[2] *National Institute for Astrophysics - Institute for Space Astrophysics and Planetology*
Via del Fosso del Cavaliere 100, 00133 Roma, Italy
[3] *National Research Council - Institute of Atmospheric Pollution Research*
c/o University of Calabria, 87036 Rende, Italy
[4] *Italian Space Agency*
Via del Politecnico snc, 00133 Roma, Italy

(Received May 27, 2020; Revised May 27, 2020; Accepted May 27, 2020)

Submitted to ApJ

ABSTRACT

This paper reports the first polarization measurement in the Alfvénic slow solar wind. The normalized magnetic helicity is used as a diagnostic parameter for studying the polarization status of the high-frequency magnetic fluctuations, with the attempt of identifying various wave modes in the solar wind turbulence. Clear evidence for the existence of Ion Cyclotron Waves (ICWs) and Kinetic Alfvén Waves (KAWs) is found also in the Alfvénic low-speed plasma, robustly supporting the idea that the Alfvénic content of the solar wind fluctuations at fluid scales is the key parameter in driving the wave generation at kinetic scales. By separating the contributions to helicity from the two modes, it is possible to address the thermodynamical properties of ICWs and KAWs and to provide the first direct estimate of their magnetic compressibility. In particular, while ICWs are mainly associated to higher levels of anisotropy and appear to be bounded by the threshold of proton-cyclotron kinetic instability, KAWs (which result to be more compressive than ICWs) are found **at lower anisotropies and seem to be limited by the mirror mode instability threshold, extending as well to near the parallel fire hose unstable region.** These result are relevant to theories of turbulence and dissipation in the solar wind.

Keywords: magnetohydrodynamics (MHD) — plasmas — polarization — turbulence — waves — solar wind

1. INTRODUCTION

The Alfvénic slow solar wind is a stream of magnetized plasma expanding in the heliosphere that, besides the self-evident difference in bulk speed, shares with the fast solar wind common characteristics, which extend from the macrostructure to the microphysics, including ion composition, spectral properties, Alfvénicity (namely the level of correlation between velocity and magnetic field fluctuations), magnetic field compressibility, and amplitude of the embedded fluctuations **(D'Amicis et al. 2019, 2020)**. Their similarity suggests that the Alfvénic low- and high-speed streams have a similar solar origin, namely the polar coronal holes. In particular, while the source of the fast wind has been identified in the core of the coronal holes (Hundhausen 1972), where the solar plasma is accelerated up to 800 km s^{-1} at about 5 $R_\odot$ (Telloni et al. 2007), the Alfvénic slow wind is thought to originate in their peripheral regions, where two mechanisms, in some sense opposite but both related to the geometry of the flux tubes channeling the wind outflows, are likely at work to slow down the expanding coronal plasma to velocities typical of the low-speed streams observed in the heliosphere: the larger superradial divergence of the magnetic field lines (with respect to that

Corresponding author: Daniele Telloni
daniele.telloni@inaf.it

characteristic of the core of polar coronal holes, Wang & Sheeley 1990; Abbo et al. 2010) and the areal narrowing of the magnetic flux tubes (Antonucci et al. 2005). In particular, since a larger superradial magnetic field geometry implies a sonic point located at higher heights, it results that in the regions adjacent to the coronal holes most of the energy deposition would occur below the sonic point, with a consequent increasing of the mass flux rather than the flow speed (as predicted by Leer & Holzer 1980), which thus retains relatively small values (Kopp & Holzer 1976; Levine et al. 1977; Wang & Sheeley 1990; Abbo et al. 2016). On the other hand, the narrowing of the cross-section of the flux tubes at the edge of polar coronal holes (that is, surrounding the streamer boundaries) from an initially high areal divergence, can lead to flow stagnation, which has the effect of slowing down the wind relative to a radial flow (Nerney & Suess 2005). **On the other hand, recent studies agree to identify possible sources of the Alfvénic slow solar wind in small coronal hole at low latitudes (Wang & Ko 2019; D'Amicis et al. 2019; Bale et al. 2019; Panasenco et al. 2020). Although the ones mentioned above are the most widely believed scenarios for the generation of the slow solar wind with a strong Alfvénic content, among alternative source regions for the typical slow wind, coronal streamers (see Abbo et al. 2016, and references therein) and active regions (Zangrilli & Poletto 2012) deserve to be mentioned.**

The discovery of the existence of a slow wind characterized by a high degree of correlation between the velocity $\mathbf{V}$ and magnetic field $\mathbf{B}$ vectors (say, $\mathbf{V}-\mathbf{B}$ correlation) dates back to the early 1980s, when Marsch et al. (1981) first identified an Alfvénic low-speed stream at 0.3 AU during the perihelion passage of the *Helios 2* mission, in a period of low solar activity. However, a statistical and rather comprehensive investigation of the Alfvénic slow wind is to be ascribed to D'Amicis & Bruno (2015) and later on to D'Amicis et al. (2019), Perrone et al. (2020) and Stansby et al. (2020), who provided a detailed characterization of this type of wind (along with its similarities with the fast wind) at both 0.3 and 1 AU and during different phases of the solar cycle. The overall properties of the Alfvénic slow wind as outlined in these studies are summarized below.

As far as large scales are considered, the Alfvénic slow wind observed at 1 AU clearly resembles the fast wind. Overall the bulk parameters (exception made for the speed and temperature, which is closer to that assumed by the typical slow wind, but including density and magnetic field intensity, along with their constant trends) are indeed very similar to those found in the main portion of high-speed streams. Moreover, both these Alfvénic solar flows are characterized by a remarkable low magnetic and density compressibility and by the same high level of $\mathbf{V}-\mathbf{B}$ correlation, typical of the presence of Alfvénic fluctuations. The Alfvénic slow wind is strongly turbulent ($\delta\mathbf{B}/B \sim 1$), with fluctuations as large as those of the fast wind (D'Amicis et al. 2020): this reflects into a similar high power level of the spectra at fluid scales. Due to the presence of highly Alfvénic fluctuations, the speed of the Alfvénic slow wind is modulated by the local magnetic field direction, similarly to what experienced by the fast wind (Matteini et al. 2014, 2015). Furthermore, the ion composition, deduced by the ratio of the oxygen (O^{7+}/O^{6+}) and carbon (C^{6+}/C^{5+}) ions, of the Alfvénic fast and slow winds is similar, suggesting a common coronal source origin**, as firstly pointed out by D'Amicis et al. (2019)**. Finally, with respect to the typical non-Alfvénic **low-speed streams**, both the Alfvénic **fast and slow winds** are characterized by lower values of the collisional age **(D'Amicis et al. 2019)**, indicating that **in the younger Alfvénic wind, the lower Coulomb collisions have less effects in isotropizing the cores of ion velocity distributions (Marsch & Goldstein 1981), which can thus preserve their non-thermal features.**

The similarities between the Alfvénic slow wind and the fast wind are not limited to the macrostructure, rather they extend also to local microphysics. Both of them occupy approximately the same region in the plasma beta-temperature anisotropy $\beta_{\parallel} - T_{\perp}/T_{\parallel}$ plane ($\beta_{\parallel}$ is the square of the ratio between the parallel thermal speed and the Alfvén speed), thus suggesting common physical processes underlying the heating of the solar wind plasma at kinetic scales. Also the small-scale phenomenology of a steeper and steeper slope of the magnetic spectrum at proton scales for a larger and larger power associated with the turbulent Alfvénic fluctuations at fluid scales (first reported by Bruno et al. 2014, for fast streams) is fully recovered also on slower streams as long as they are Alfvénic. Furthermore, as already shown for the fast wind (Bruno & Trenchi 2014), also in the Alfvénic slow wind the location of the high-frequency break separating fluid from kinetic scales is well predicted by a cyclotron resonance condition**, as firstly reported by D'Amicis et al. (2019) and later on by Duan et al. (2020) on the recent results of the *Parker Solar Probe***. These last two observational evidences are of particular interest since they are both strictly related to the mechanism acting in the solar wind to heat the plasma.

It has been indeed recently shown on a statistical basis (Telloni et al. 2019) that the amplitude of the Alfvénic fluctuations at fluid scales, rather than the solar wind speed, is the key parameter in driving the generation of

Ion Cyclotron Waves (ICWs) at kinetic scales through proton cyclotron instability, triggered by large temperature anisotropies. ICWs can be thus interpreted as the most evident signature of the resonant dissipation of high-frequency Alfvén waves at frequencies near the gyrofrequency $\Omega_p = qB/(m_p c)$ (q and m_p are the proton electric charge and rest mass, respectively, B is the magnetic field intensity, and c is the speed of light). **As a matter of fact, He et al. (2019) directly measured the dissipation rate spectrum of the ICWs in the magnetosheath turbulence.** Similarly, it is reasonable to assume that the Alfvénicity is the major parameter in regulating also the signature of the Kinetic Alfvén Waves (KAWs). As a matter of fact, Bruno & Telloni (2015) provided clues in favor of this conjecture, showing that KAWs are indeed gradually depleted moving, along a high-speed stream, from the more Alfvénic fast wind to the rarefaction region, where the Alfvénicity of the low-frequency fluctuations decreases. Hence, if it were possible to provide evidence for the existence of ICWs and KAWs also in the Alfvénic slow wind, it would be definitely proven that their presence in the solar wind plasma is not related to the nature of the flow (i.e. fast or slow), but rather to its degree of Alfvénicity. It would follow that the generation at kinetic scales of ICWs and KAWs is driven by the solar wind properties at fluid scales, thus supporting previous suggestions by Telloni & Bruno (2016) and Telloni et al. (2019). However, such an information is still missing in the present literature: this motivates the investigation of the presence of ICWs and KAWs in the Alfvénic slow solar wind, which is the aim of this paper.

Since ICWs and KAWs are circularly polarized waves with frequencies $\sim \Omega_p$, their identification requires the use of normalized magnetic helicity σ_m, defined as (Matthaeus et al. 1982; Matthaeus & Goldstein 1982)

$$\sigma_m(\omega) = \frac{2\,\mathrm{Im}[Y^*(\omega)\cdot Z(\omega)]}{E_B}, \tag{1}$$

where Y and Z are the Fourier transforms of the y and z components of B (as a function of the frequency ω), and E_B is the total magnetic spectral energy. The normalized magnetic helicity σ_m quantifies indeed the handedness of the magnetic field fluctuations ($\sigma_m = \pm 1$ for right- and left-circularly polarized waves), allowing the characterization of the polarization state of the solar wind parallel and perpendicular fluctuations at proton scales. The data analysis, presented in § 2, is essentially based on the study of distribution of σ_m at kinetic scales as a function of the angle between the solar wind velocity and the local mean magnetic field vectors θ_{VB}, and in the plasma beta-temperature anisotropy $\beta_\parallel - T_\perp/T_\parallel$ and **VB angle**-magnetic compressibility $\theta_{VB} - C_B$ planes. Discussion of the obtained results and concluding remarks are reported in § 3.

2. ANALYSIS AND RESULTS

The analysis is performed on the Alfvénic low-speed stream observed at 1 AU from 26 to 30 of January 2002, already subject of investigation in the works by D'Amicis & Bruno (2015) and D'Amicis et al. (2019). Some relevant solar wind parameters relative to this time interval are shown, among with the corresponding average values, in the hatched red area of Fig. 1, which altogether extends from January 22, **2002** to February 03, 2002. The figure panels display the time profiles of the solar wind speed V, the $\mathbf{V}-\mathbf{B}$ correlation coefficient ρ_{VB} computed at 1-hour scale (since this scale is characterized by strong Alfvénic solar wind fluctuations, Bruno et al. 1997), magnetic field intensity B, proton number density n_p and temperature T_p, total pressure P, proton temperature anisotropy $T_\perp/T_\parallel$, and parallel proton plasma beta $\beta_\parallel$. Data come from the Magnetic Field Investigation (MFI) magnetometer (Lepping et al. 1995) and the Solar Wind Experiment (SWE) instrument (Ogilvie et al. 1995) onboard the *Wind* spacecraft, which provide high-resolution 11 Hz magnetic field measurements and 92-second resolution moments from proton velocity distribution functions, respectively.

Although the large-scale properties of this Alfvénic slow flow have been exhaustively described in the previous studies by D'Amicis & Bruno (2015) and D'Amicis et al. (2019), it is worth recalling its main characteristics as outlined by Fig. 1. The $\mathbf{V}-\mathbf{B}$ correlation coefficient ρ_{VB}, which quantifies the Alfvénic content of the solar wind fluctuations, retains very high values along the whole low-speed stream ($\langle\rho_{VB}\rangle = 0.91$), thus robustly indicating the presence of Alfvénic fluctuations (panel b)). As expected for Alfvénic flow streams, also this Alfvénic time period is characterized by enhanced velocity fluctuations, and by low compression in both magnetic field intensity and proton number density (panels a), c) and d), respectively). The temperature and pressure observed within the Alfvénic slow flow are larger than in the upstream and downstream regions (panels e) and f), respectively), likely indicating that **the flux-tube expansion factor is larger** with respect to the surrounding plasma, in accordance with the superradial expansion as the major mechanism responsible for the lower speeds. Finally, a low level of temperature anisotropy ($\langle T_\perp/T_\parallel\rangle = 1.62$) and a plasma-magnetic pressure imbalance ($\langle\beta_\parallel\rangle = 0.21$) is observed (panels g) and h), respectively). In particular,

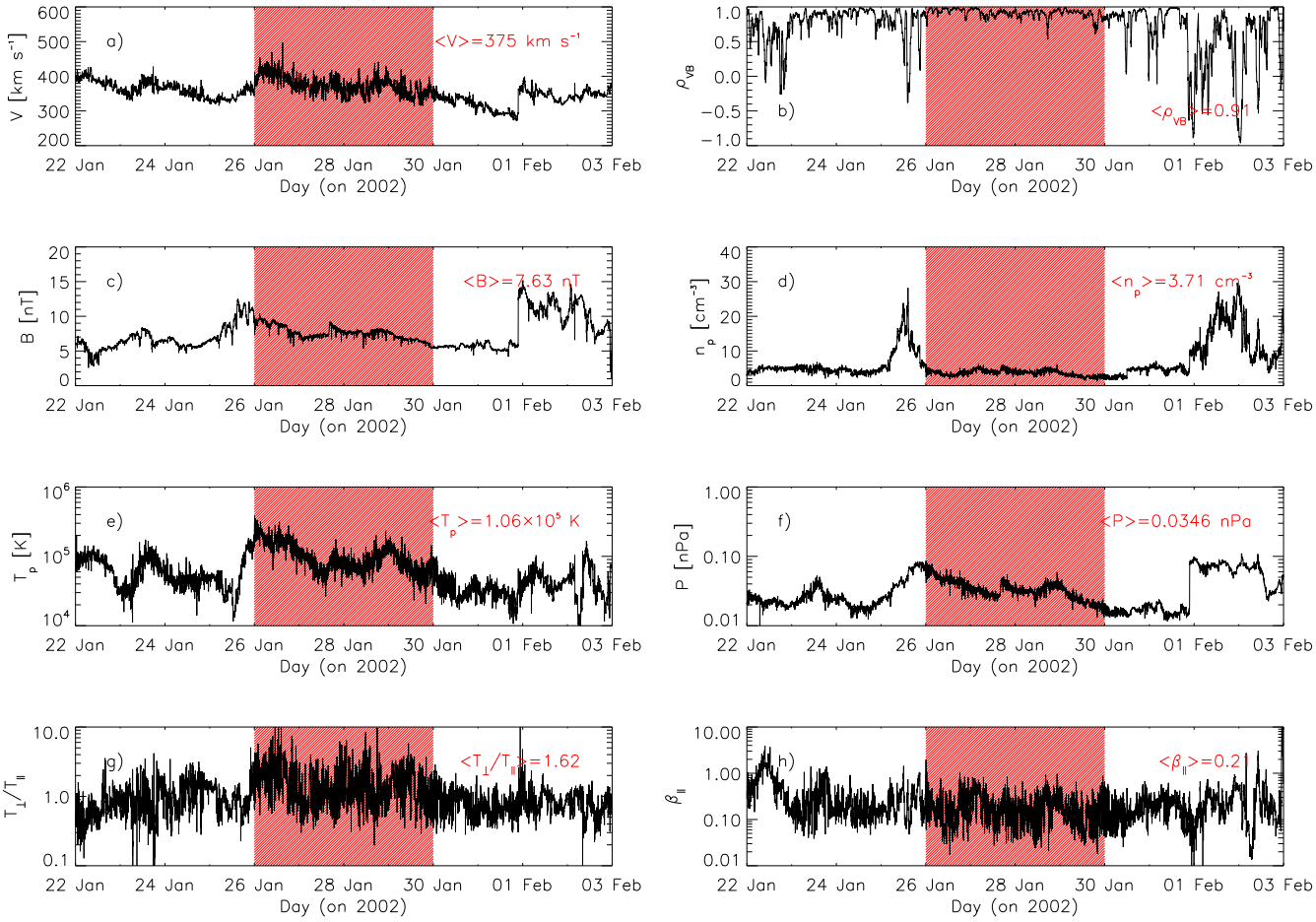

Figure 1. Time series of solar wind speed (a), $\mathbf{V}-\mathbf{B}$ correlation coefficient (b), magnetic field intensity (c), proton number density (d) and temperature (e), total pressure (f), proton temperature anisotropy (g), and parallel proton plasma beta (h), over the period from January 22, 2002 to February 03, 2002; the hatched red area highlights the Alfvénic low-speed stream under study; the corresponding average values of the solar wind parameters are reported in each panel.

these last two parameters are very important (since they allow the description of the thermodynamical state of the plasma) and will be used to investigate of the nature of the polarized magnetic fluctuations at proton scales.

In order to search for the existence of ICWs and KAWs in the Alfvénic slow wind, the approach of using the normalized magnetic helicity σ_m to diagnose the wave-polarization characteristics of the magnetic field fluctuations (first introduced by He et al. 2011; Podesta & Gary 2011) is adopted in this work. It is based on the estimation of the θ_{VB} distribution of σ_m at every frequency and on the search for populations of field-aligned (highly oblique) fluctuations with an intrinsic negative (positive) magnetic helicity sign ($\sigma_m \lessgtr 0$), at frequencies near the gyrofrequency Ω_p, which can be indeed interpreted as parallel-(perpendicular-)propagating left-(right-)handed polarized ICWs (KAWs). More details on this analysis technique can be found in previous literature (e.g. He et al. 2011; Podesta & Gary 2011; Telloni et al. 2015; Bruno & Telloni 2015).

The results of this polarization analysis are shown in Fig. 2, which displays the distribution of the normalized magnetic helicity σ_m as a function of the local **VB angle** and frequency.

Two strongly and oppositely polarized magnetic populations are clearly resolved just below the proton cyclotron resonance frequency Ω_p (dashed line in Fig. 2), at quasi-perpendicular and quasi-parallel directions. Since the magnetic sector observed during the selected time interval is inwardly oriented, the positive (negative) magnetic helicity excesses shown in the σ_m angular distribution, correspond to left- and right-handed polarized fluctuations, which are respectively propagating roughly along and across the local magnetic field. These magnetic fluctuations are commonly interpreted

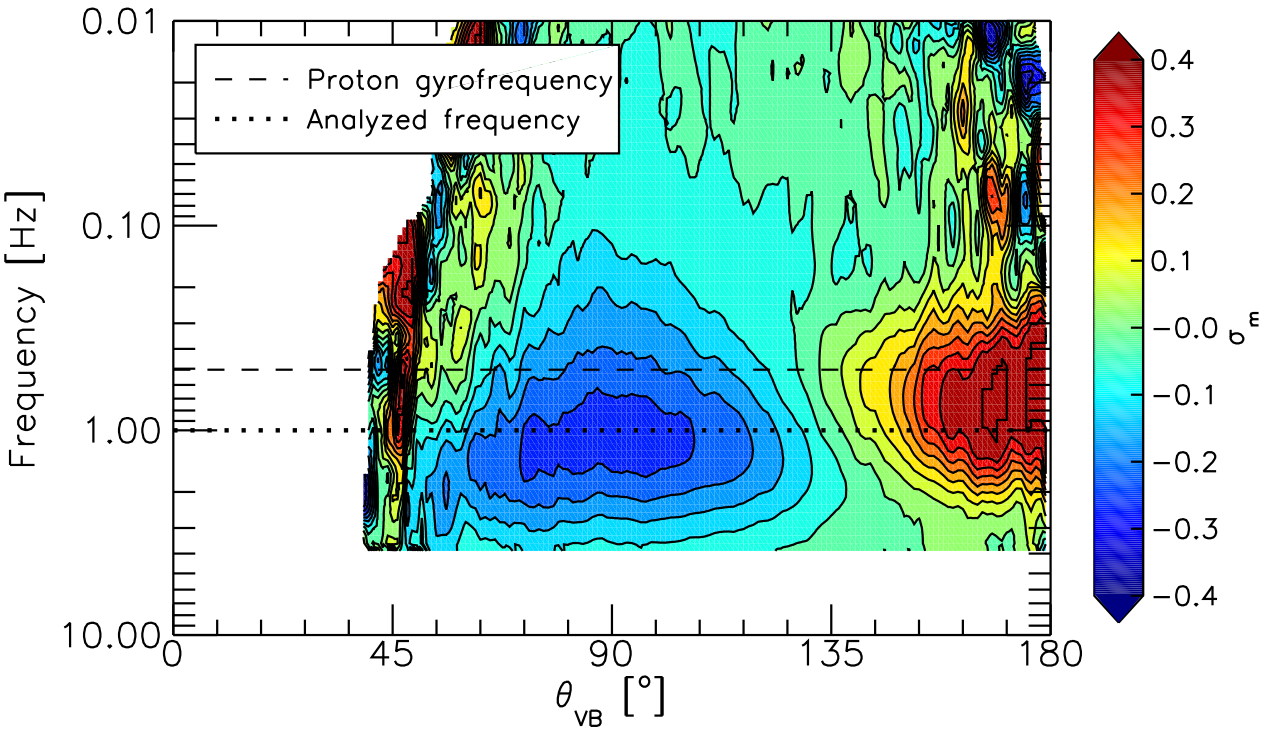

Figure 2. Distribution of the normalized magnetic helicity σ_m spectrum with respect to the θ_{VB} angle between the flow direction and the local mean magnetic field; the frequency corresponding to the proton cyclotron resonance condition and that selected for analyzing the nature of the polarized fluctuations at proton scales (see text for details) are shown as a dashed and dotted line, respectively.

as due to Kinetic Alfvén Waves (KAWs) and ICWs (He et al. 2011; Podesta & Gary 2011; Telloni et al. 2015; Bruno & Telloni 2015; Telloni & Bruno 2016), which thus transpire to exist also in Alfvénic slow wind. Quite interestingly, as already noticed in Telloni et al. (2015) and Bruno & Telloni (2015) for the fast wind, also in the Alfvénic slow wind the core of the ICW population is located at lower frequencies with respect to that of KAWs, which have moreover a larger frequency extend.

In order to characterize in more details these two families of magnetic fluctuations of which the selected Alfvénic low-speed stream is made of, the contribution to normalized magnetic helicity from ICWs and KAWs is separated, by studying the distribution of σ_m in the plasma beta-temperature anisotropy $\beta_{\parallel} - T_{\perp}/T_{\parallel}$ and in the **VB angle**-magnetic compressibility $\theta_{VB} - C_B$ spaces. In order to accomplish this task, the frequency of 1 Hz, which runs close to the cores of the two oppositely polarized populations (dotted line in Fig. 2) thus allowing the capture of both ICWs and KAWs, is considered in the analysis. The left and right panels of Fig. 3 show the median values of σ_m at 1 Hz in the $\beta_{\parallel} - T_{\perp}/T_{\parallel}$ and $\theta_{VB} - C_B$ parameter planes, respectively. The four plasma instabilities driven by proton temperature anisotropy (as adapted from Hellinger et al. 2006, for a constant maximum growth rate $\gamma \sim 10^{-3}\Omega_p$) are displayed in the $\beta_{\parallel} - T_{\perp}/T_{\parallel}$ space with different line types.

As highlighted in D'Amicis et al. (2019), when the Alfvénic low-speed stream of January 2002 is studied as a whole, the plasma is on average in a thermodynamical state characterized by an almost thermal equilibrium ($T_{\perp}/T_{\parallel} \sim 1$) and by low beta values ($\beta_{\parallel} \sim 0.3$). Furthermore, overall a very low compressibility is exhibited by the magnetic fluctuations,

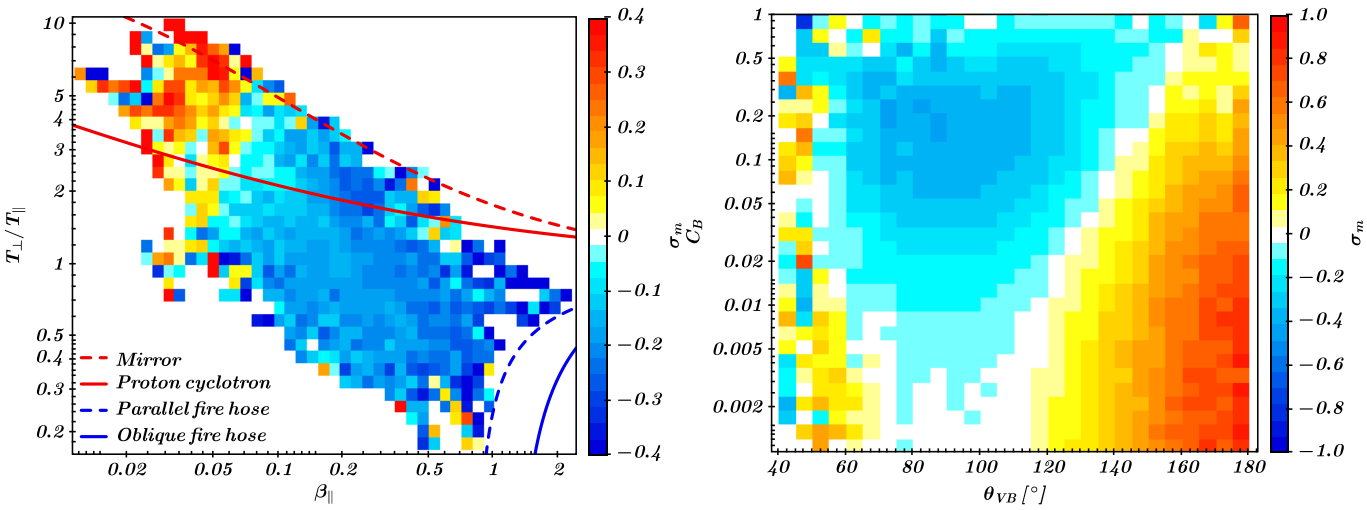

Figure 3. 2D histogram of the median value of the normalized magnetic helicity σ_m in the $\beta_\parallel - T_\perp/T_\parallel$ (*left*) and $\theta_{VB} - C_B$ (*right*) spaces; the mirror, proton, and parallel and oblique fire hose instabilities are also reported in the $\beta_\parallel - T_\perp/T_\parallel$ plane as lines with different styles.

as expected for highly Alfvénic intervals (Bruno & Bavassano 1991). However, the separation of the ICWs and KAWs on the basis of their polarization gives the possibility to estimate their correlation with the thermodynamical state of plasma and their compressibility level. The two populations are indeed clearly distinguishable in both the $\beta_\parallel - T_\perp/T_\parallel$ and $\theta_{VB} - C_B$ planes. ICWs are found at high temperature anisotropies ($T_\perp/T_\parallel \gtrsim 3$) and very low beta plasma values ($\beta_\parallel \lesssim 0.07$), *de facto* in a region unstable with respect to the proton cyclotron instability (as already reported by Telloni et al. 2015, 2019, for the fast wind). On the other hand, KAWs are distributed in a much larger region of the $\beta_\parallel - T_\perp/T_\parallel$ space, where $\beta_\parallel$ is generally smaller than 0.1 and $T_\perp/T_\parallel$ mostly lower than 1. The wide intervals of $T_\perp/T_\parallel$ and $\beta_\parallel$ values spanned by KAWs might indicate that these fluctuations are somehow insensitive to proton temperature anisotropy, in agreement with Klein & Howes (2015). However, KAWs seem to be possibly limited by the parallel fire hose instability (blue dashed line in the left panel of Fig. 3), which can be thus suggested to play some role in driving modes with a right-handed helicity**, even if no definitive conclusions can be drawn only on the basis of the present analysis. Indeed, there is currently no theory predicting that KAWs are directly excited by the fire hose instability. At fluid scales, the fire hose instability can be responsible for the generation of Alfvén waves, as reported for instance by He et al. (2018) in the magnetic reconnection exhaust regions, where enhanced Alfvénic turbulence has been observed in relation to fire hose unstable energized plasmas. At kinetic scales, it is predicted that the fire hose instability drives quasi-parallel propagating and right-handed polarized wave modes, thus interpreted as magnetosonic/whistler waves (e.g. Podesta & Gary 2011). On the other hand, KAWs may be excited by electron current instability or energetic ion beam instability (Voitenko 1998; Chen et al. 2013). Furthermore, observations show that KAWs lie inside the region unstable with respect to the proton cyclotron instability and seem to be bounded also by the mirror mode instability threshold (red solid and dashed lines in the left panel of Fig. 3, respectively). Therefore, which plasma instability is crucial in driving KAWs or whether more instabilities may be at play at the same time are still open questions, which require further observational and theoretical investigation to be tackled.**

In addition, this technique allows, for the first time in literature, the estimation of the compressive character of ICWs and KAWs. In fact, the right panel of Fig. 3 indicates that right-handed polarized fluctuations ($\sigma_m < 0$) propagating at $\theta_{VB} \sim 90°$ have a compressive ratio $C_B = \left(\sigma_B^2 / \sum_{i=x,y,z} \sigma_{B_i}^2\right)^{1/2}$ (with σ_B^2 and $\sigma_{B_i}^2$ the variances of the magnetic field intensity and components, respectively, computed over 1 second) of about 0.1 or more, while parallel-propagating left-handed polarized fluctuations ($\sigma_m > 0$) exhibit much lower values ($C_B \lesssim 0.01$). It thus transpires that KAWs are largely more compressive than ICWs. As a matter of fact, as the wavevector $\mathbf{k}$ becomes relatively more and more oblique to the background magnetic field, compressibility increases consequently. Thus, it is experimentally confirmed

that most of the compressive character of the fluctuations at proton kinetic scales (e.g. Hollweg 1999; Alexandrova et al. 2008; Podesta 2013; Telloni et al. 2015, and many others) is mainly due to the presence of KAWs.

3. DISCUSSION AND CONCLUSIONS

The results outlined in the previous section show that ICWs and KAWs populate also the slow wind as long as it is characterized by a high degree of Alfvénic correlations. Hence, the presence of Alfvén waves in the inertial range is a *sine qua non* condition for the existence of both these types of waves at kinetic scales in the solar wind turbulence. This is a further evidence that the solar wind should be classified according to its Alfvénicity level, rather than to its speed. In other words, the classic distinction in fast and slow wind should be revised in Alfvénic and not Alfvénic streams. Indeed, as exhaustively shown by D'Amicis et al. (2019), the Alfvénic slow wind shares much more characteristics with the fast wind than with the typical, not Alfvénic slow flow. This paper extends their similarities to the thermodynamical properties of ICWs and KAWs. A comparison of the left panel of Fig. 3 with Fig. 3 reported in Telloni & Bruno (2016) clearly reveals that in both fast and slow Alfvénic solar wind regimes, ICWs occupy approximately the same region in the $\beta_{\parallel} - T_{\perp}/T_{\parallel}$ parameter space, at $T_{\perp}/T_{\parallel} > 1$ and $\beta_{\parallel} < 1$, exhibiting a higher temperature anisotropy and a lower parallel plasma beta with respect to KAWs. Similarly, KAWs are mainly located around $T_{\perp}/T_{\parallel} \sim 1$ and $\beta_{\parallel} \sim 1$ in both wind types.

Although some clues were already provided by Telloni et al. (2015), this paper reports also the first experimental assessment of the compressibility level of ICWs and KAWs, with the latter resulting much more compressive than the former. The low (high) magnetic compressibility exhibited by $k_{\parallel}$ ($k_{\perp}$) fluctuations at frequencies around Ω_p reinforces their interpretation in terms of ICWs and KAWs, respectively. As turbulence develops for $\mathbf{k}_{\perp}$, Alfvénic fluctuations at kinetic scales have very oblique wavevectors and are hence very compressive. Thus, as a further result, this paper observationally supports those theoretical models predicting that high-frequency magnetic fluctuations in a low-beta solar wind plasma mainly arise from a spectrum of KAWs (Howes et al. 2008; Schekochihin et al. 2009).

DT and RDM were partially supported by the Italian Space Agency (ASI) under contract I/013/12/0. *Wind* data were downloaded from the NASA-CDAWeb.

REFERENCES

Abbo, L., Antonucci, E., Mikić, Z., et al. 2010, AdSpR, 46, 1400

Abbo, L., Ofman, L., Antiochos, S. K., et al. 2016, SSRv, 201, 55

Alexandrova, O., Carbone, V., Veltri, P., & Sorriso-Valvo, L. 2008, ApJ, 674, 1153

Antonucci, E., Abbo, L., & Dodero, M. A. 2005, A&A, 435, 699

Bale, S. D., Badman, S. T., Bonnell, J. W., et al. 2019, Nature, 576, 237

Bruno, R., & Bavassano, B. 1991, J. Geophys. Res., 96, 7841

Bruno, R., Bavassano, B., Pietropaolo, E., Carbone, V., & Rosenbauer, H. 1997, J. Geophys. Res., 102, 14687

Bruno, R., & Trenchi, L. 2014, ApJL, 787, L24

Bruno, R., Trenchi, L., & Telloni, D. 2014, ApJL, 793, L15

Bruno, R., & Telloni, D. 2015, ApJL, 811, L17

Chen, L., Wu, D. J., & Huang, J. 2013, J. Geophys. Res., 118, 2951

D'Amicis, R., & Bruno, R. 2015, ApJ, 805, 84

D'Amicis, R., Matteini, L., & Bruno, R. 2019, MNRAS, 483, 4665

D'Amicis, R., Matteini, L., Bruno, R., & Velli, M. 2020, SoPh, 295, 46

Duan, D., Bowen, T. A., Chen, C. H. K., et al. 2020, ApJS, 246, 55

He, J., Marsch, E., Tu, C., Yao, S., & Tian, H. 2011, ApJ, 731, 85

He, J., Zhu, X., Chen, Y., et al. 2018, ApJ, 856 148

He, J., Duan, D., Wang, T., et al. 2019, ApJ, 880, 121

Hellinger, P., Trávníček, P., Kasper, J. C., & Lazarus, A. J. 2006, Geophys. Res. Lett., 33, L09101

Hollweg, J. V. 1999, J. Geophys. Res., 104, 14811

Howes, G. G., Dorland, W., Cowley, S. C., et al. 2008, PhRvL, 100, 065004

Hundhausen, A. J. 1972, Coronal Expansion and Solar Wind (New York: Springer)

Klein, K. G., & Howes, G. G. 2015, PhPl, 22, 032903

Kopp, R. A., & Holzer, T. E. 1976, SoPh, 49, 43

Leer, E., & Holzer, T. E. 1980, J. Geophys. Res., 85, 4681

Lepping, R. P., Acũna, M. H., Burlaga, L. F., et al. 1995, SSRv, 71, 207

Levine, R. H., Altschuler, M. D., Harvey, J. W., & Jackson, B. V. 1977, ApJ, 215, 636

Marsch, E., Rosenbauer, H., Schwenn, R., R., Muehlhaeuser, K.-H., & Denskat, K. U. 1981, J. Geophys. Res., 86, 9199

Marsch, E., & Goldstein, H. 1983, J. Geophys. Res., 88, 9933

Matteini, L., Horbury, T. S., Neugebauer, M., & Goldstein, B. E. 2014, Geophys. Res. Lett., 41, 259

Matteini, L., Horbury, T. S., Pantellini, F., Velli, M., & Schwartz, S. J. 2015, ApJ, 802, 11

Matthaeus, W. H., Goldstein, M. L., & Smith, C. 1982, PhRvL, 48, 1256

Matthaeus, W. H., & Goldstein, M. L. 1982, J. Geophys. Res., 87, 6011

Nerney, S., & Suess, S. T. 2005, ApJ, 624, 378

Ogilvie, K., Chornay, D., Fritzenreiter, R., et al. 1995, SSRv, 71, 55

Panasenco, O., Velli, M., D'Amicis, R., et al. 2020, ApJS, 246, 54

Perrone, D., D'Amicis, R., De Marco, R., et al. 2020, A&A, 633, A166

Podesta, J. J., & Gary, S. P. 2011, ApJ, 734, 15

Podesta, J. J. 2013, SoPh, 286, 529

Schekochihin, A. A., Cowley, S. C., Dorland, W., et al. 2009, ApJS, 182, 310

Stansby, D., Matteini, L., Horbury, T. S., et al. 2020, MNRAS, 492, 39

Telloni, D., Antonucci, E., & Dodero, M. A. 2007, A&A, 472, 299

Telloni, D., Bruno, R., & Trenchi, L. 2015, ApJ, 805, 46

Telloni, D., & Bruno, R. 2016, MNRAS, 463, L79

Telloni, D., Carbone, F., Bruno, R., et al. 2019, ApJL, 885, L5

Voitenko, Yu. M. 1998, JPlPh, 60, 497

Wang, Y.-M., & Sheeley, N. R., Jr. 1990, ApJ, 355, 726

Wang, Y.-M., & Ko, Y.-K. 2019, ApJ, 880, 146

Zangrilli, L., & Poletto, G. 2012, A&A, 545, A8